ELSEVIER

Stereochemistry of the insertion of disubstituted alkynes into the metal aminocarbyne bond in diiron complexes

Vincenzo G. Albano [a], Luigi Busetto [b], Fabio Marchetti [b], Magda Monari [a], Stefano Zacchini [b], Valerio Zanotti [b],*

[a] *Dipartimento di Chimica "G. Ciamician", Università di Bologna, Via Selmi 2, I-40126 Bologna, Italy*
[b] *Dipartimento di Chimica Fisica ed Inorganica, Università di Bologna, Viale Risorgimento 4, I-40136 Bologna, Italy*

Abstract

Terminal alkynes (HC≡CR$'$) (R$'$ = COOMe, CH$_2$OH) insert into the metal–carbyne bond of the diiron complexes [Fe$_2$\{μ-CN(Me)(R)\}(μ-CO)(CO)(NCMe)(Cp)$_2$][SO$_3$CF$_3$] (R = Xyl, **1a**; CH$_2$Ph, **1b**; Me, **1c**; Xyl = 2,6-Me$_2$C$_6$H$_3$), affording the corresponding μ-vinyliminium complexes [Fe$_2$\{μ-σ:η^3-C(R$'$)=CHC=N(Me)(R)\}(μ-CO)(CO)(Cp)$_2$][SO$_3$CF$_3$] (R = Xyl, R$'$ = COOMe, **2**; R = CH$_2$Ph, R$'$ = COOMe, **3**; R = Me, R$'$ = COOMe, **4**; R = Xyl, R$'$ = CH$_2$OH, **5**; R = Me, R$'$ = CH$_2$OH, **6**). The insertion is regiospecific and C–C bond formation selectively occurs between the carbyne carbon and the CH moiety of the alkyne. Disubstituted alkynes (R$'$C≡CR$'$) also insert into the metal–carbyne bond leading to the formation of [Fe$_2$\{μ-σ:η^3-C(R$'$)=C(R$'$)C=N(Me)(R)\}(μ-CO)(CO)(Cp)$_2$][SO$_3$CF$_3$] (R$'$ = Me, R = Xyl, **8**; R$'$ = Et, R = Xyl, **9**; R$'$ = COOMe, R = Xyl, **10**; R$'$ = COOMe, R = CH$_2$Ph, **11**; R$'$ = COOMe, R = Me, **12**). Complexes **2**, **3**, **5**, **8**, **9** and **11**, in which the iminium nitrogen is unsymmetrically substituted, give rise to *E* and/or *Z* isomers. When iminium substituents are Me and Xyl, the NMR and structural investigations (X-ray structure analysis of **2** and **8**) indicate that complexes obtained from terminal alkynes preferentially adopt the *E* configuration, whereas those derived from internal alkynes are exclusively *Z*. In complexes **8** and **9**, *trans* and *cis* isomers have been observed, by NMR spectroscopy, and the structures of *trans*-**8** and *cis*-**8** have been determined by X-ray diffraction studies. *Trans* to *cis* isomerization occurs upon heating in THF at reflux temperature. In contrast to the case of HC≡CR$'$, the insertion of 2-hexyne is not regiospecific: both [Fe$_2$\{μ-σ:η^3-C(CH$_2$CH$_2$CH$_3$)=C(Me)C=N(Me)(R)\}(μ-CO)(CO)(Cp)$_2$][SO$_3$CF$_3$] (R = Xyl, **13**; R = Me, **15**) and [Fe$_2$\{μ-σ:η^3-C(Me)=C(CH$_2$CH$_2$CH$_3$)C=N(Me)(R)\}(μ-CO)(CO)(Cp)$_2$][SO$_3$CF$_3$] (R = Xyl, **14**, R = Me, **16**) are obtained and these compounds are present in solution as a mixture of *cis* and *trans* isomers, with predominance of the former.
© 2003 Elsevier B.V. All rights reserved.

Keywords: Alkyne insertion; Carbyne; Vinyliminium; Diiron complexes; Crystal structure

1. Introduction

We have recently shown [1] that terminal alkynes (HC≡CR$'$) insert into the metal–carbon bond of diiron μ-aminocarbynes [Fe$_2$\{μ-CN(Me)(R)\}(μ-CO)(CO)(NCMe)(Cp)$_2$][SO$_3$CF$_3$] (R = Xyl, **1a**; CH$_2$Ph, **1b**; Me, **1c**; Xyl = 2,6-Me$_2$C$_6$H$_3$), affording the complexes [Fe$_2$\{μ-σ:η^3-C(R$'$)=CHC=N(Me)(R)\}(μ-CO)(CO)(Cp)$_2$][SO$_3$CF$_3$] (R$'$ = SiMe$_3$, Me, Bu^n, *p*-Tol, Ph, H) (Scheme 1), which contain a vinyliminium ligand in a rather unusual bridging coordination mode [2].

These reactions, providing C–C bond formation at the μ-aminocarbyne carbon [3], represent a remarkable result of our ongoing studies on the reactivity of diiron μ-aminocarbyne complexes containing nitrile ligands [4]. Interestingly, the insertion of primary alkynes is regiospecific: in all of the cases examined, the C–C bond was formed between the bridging aminocarbyne and the unsubstituted acetylene carbon, placing the more hindered R$'$ group far from the iminium moiety (Scheme 1). If the substituents at the iminium nitrogen are not identical (R≠Me), isomers originate by their different orientation with respect to the C=N double bond. In particular, when R = Xyl, the preferred orientation is that with Xyl *cis* to C$_\beta$. Insertion of disubstituted

* Corresponding author. Tel.: +39-512-093700; fax: +39-512-093690.
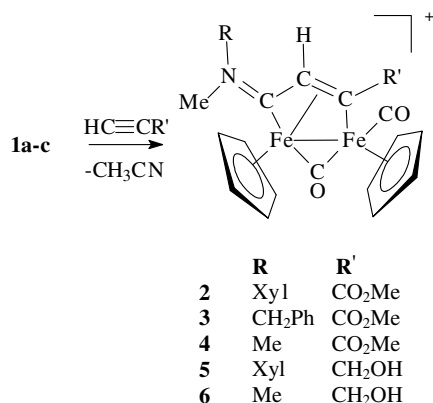*E-mail address:* zanotti@ms.fci.unibo.it (V. Zanotti).
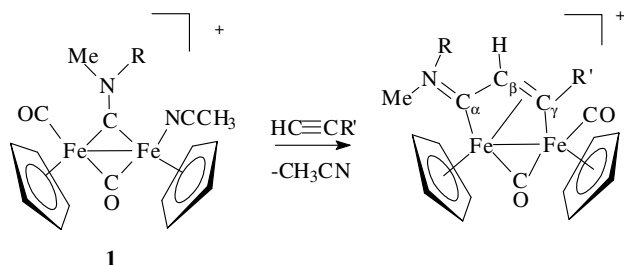
Scheme 1.

acetylenes has also been described, although limited to the symmetrically disubstituted $R'C{\equiv}CR'$ (R' = Me, Et) [1]. Herein, we present an extension of our studies to primary alkynes containing functional groups (CO_2Me, CH_2OH), and unsymmetrically disubstituted alkynes. The aim is to establish to what extent the insertion reaction is influenced by the steric hindrance and nature of the acetylene substituents. Finally we want to study in more details the stereo- and regio-chemistry of the insertion reaction.

2. Results and discussion

2.1. Insertion of monosubstituted alkynes

The reactions of $[Fe_2\{\mu\text{-}CN(Me)(R)\}(\mu\text{-}CO)(CO)(NCMe)(Cp)_2][SO_3CF_3]$ (**1a–c**) with monosubstituted acetylenes $HC{\equiv}CR'$ containing a functional group (R' = CO_2Me, CH_2OH), are performed in CH_2Cl_2 solution heated at refluxing temperature for 4 h, and result in the formation of the complexes $[Fe_2\{\mu\text{-}\sigma{:}\eta^3\text{-}C(R')=CHC=N(Me)(R)\}(\mu\text{-}CO)(CO)(Cp)_2][SO_3CF_3]$ (**2–6**) (Scheme 2). The presence of functional groups (hydroxy or carboxylate) in the alkyne does not affect its insertion into the metal–carbyne bond, which occurs as previously described [1].

Compounds **2–6** have been obtained in good yields (60–85%), and characterized by spectroscopy and ele-

mental analyses. Moreover, the complex $[Fe_2\{\mu\text{-}\sigma{:}\eta^3\text{-}C(CO_2Me)=CHC=N(Me)(Xyl)\}(\mu\text{-}CO)(CO)(Cp)_2][SO_3CF_3]$ (**2**) has been structurally characterized by an X-ray diffraction study and the structure of the cation is shown in Fig. 1. The stereogeometry is that expected and equivalent both in conformation and bond values to that just reported for $[Fe_2\{\mu\text{-}\sigma{:}\eta^3\text{-}C(SiMe_3)=CHC=N(Me)(Xyl)\}(\mu\text{-}CO)(CO)(Cp)_2]^+$ [1], in which the $SiMe_3$ group takes the place of CO_2Me. Orientation of the iminium substituents corresponds to the *E*-isomer (Scheme 3), with the Xyl group pointing far from the Cp ligand. Relevant bond parameters are listed in Table 1 and the only comment is that the substituent groups do not have significant effects on the molecular conformation and bond distances.

The insertion of $HCCR'$ into the Fe–C bond reported in Scheme 2 is regiospecific and the CR' termination (R' = CO_2Me, CH_2OH) is bound exclusively to Fe, presumably to avoid steric interactions with the N-substituents. This is indicated in the ^1H NMR spectra of **2–6**, by the observed resonance in the range 3.9–5.5 ppm, which is attributable to $C_\beta H$. Furthermore, no signal is detected in the low field range expected for a
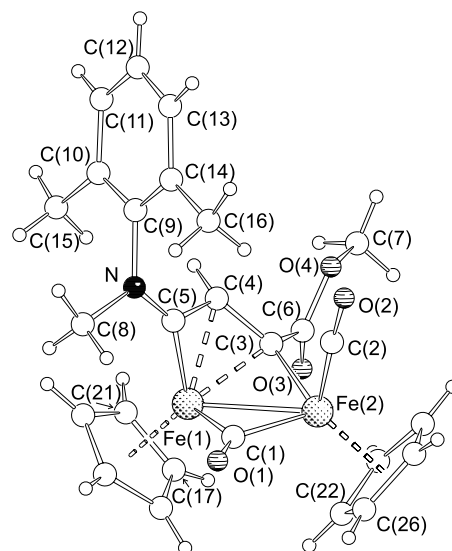
Fig. 1. Molecular structure of the cation of $[Fe_2\{\mu\text{-}\sigma{:}\eta^3\text{-}C(CO_2Me)=CHC=N(Me)(Xyl)\}(\mu\text{-}CO)(CO)(Cp)_2][SO_3CF_3]$ (**2**). Only the main image of the disordered Cp ligand bound to Fe(2) is drawn.

	R	R'
2	Xyl	CO_2Me
3	CH_2Ph	CO_2Me
4	Me	CO_2Me
5	Xyl	CH_2OH
6	Me	CH_2OH
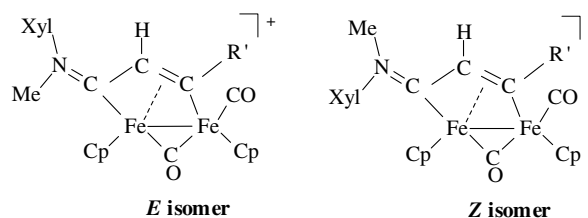
Scheme 2.

Scheme 3.

Table 1
Selected bond lengths (Å) and angles (°) for **2**

Fe(1)–Fe(2)	2.549(1)	C(8)–N	1.465(8)
Fe(1)–C(3)	2.017(6)	C(9)–N	1.467(1)
Fe(1)–C(4)	2.081(6)	C(3)–C6	1.492(9)
Fe(1)–C(5)	1.843(6)	C(6)–O(4)	1.325(8)
Fe(1)–C(1)	1.954(7)	C(6)–O(3)	1.177(8)
Fe(2)–C(1)	1.929(7)	O(4)–C(7)	1.454(9)
C(1)–O(1)	1.155(8)	Fe(2)–C(2)	1.750(9)
Fe(2)–C(3)	1.954(6)	C(2)–O(2)	1.137(9)
C(3)–C(4)	1.396(8)	Fe(1)–C(Cp)(av)	2.096
C(4)–C(5)	1.421(8)	Fe(2)–C(Cp)(av)[a]	2.126
C(5)–N	1.289(7)		
C(9)–N–C(5)	121.7(5)	Fe(1)–C(5)–C(4)	78.0(3)
C(5)–C(4)–C(3)	116.3(5)	C(5)–N–C(8)	121.8(5)
N–C(5)–C(4)	133.5(5)	C(8)–N–C(9)	116.4(4)
Fe(2)–C(3)–C(4)	125.3(4)		

[a] Referred to the main image of the Cp ligand.

$C_\gamma H$ (at about 12 ppm) which would be generated by the opposite insertion mode [1,5].

The NMR spectra of **2**, **3** and **5** reveal the presence in solution of two isomers (*E* and *Z*) generated by different orientations of the Me and R substituents in the iminium moiety. Accordingly, complexes **4** and **6** having identical N substituents, exhibit one isomer only. In compounds **2** and **5** containing nitrogen substituents (Xyl and Me) with different steric hindrance, the *E*-isomer (Scheme 3, and Fig. 1) largely prevails. As previously shown [1], the ^{1}H NMR data allow to distinguish between *E* and *Z* forms, because the N–Me resonance in the *E* isomer usually falls in the range 4.1–4.3 ppm, whereas it appears about 0.7 ppm upfield shifted (in the 3.4–3.6 ppm range) in the *Z* form. Moreover, NOE studies on the major isomer of complex **2** confirm that the methyl group on the nitrogen points far from the C_β–H and close to one Cp ligand; indeed irradiation of the N–Me resonance (4.05 ppm) resulted in small but significant NOE enhancements of the resonances due to one Cp ligand (5.34 ppm) and the two methyl groups on the Xyl ring (2.29 and 1.73 ppm), whereas no effect has been detected on the resonance due to the C_β–H.

The ^{13}C NMR spectra of **2–6** exhibit resonances for the C_α, C_β and C_γ carbons (e.g. for **4** at 223.1, 51.9 and 183.2 ppm, respectively) that are similar to those previously reported for analogous vinyliminium complexes [1]: some slight differences are in line with the electron-withdrawing character of the R' substituent.

The reactions shown in Scheme 2 indicate a route for introducing functional groups at Cγ of the bridging vinyliminium ligand. This would potentially allow the synthesis of a variety of new interesting complexes. For example, compound **5** reacts with ClSiMe₃ in the presence of NEt₃, yielding the complex [Fe₂{μ-σ:η³-C(CH₂OSiMe₃)=CHC=N(Me)(Xyl)}(μ-CO)(CO)(Cp)₂][SO₃CF₃] (**7**) (Scheme 4). Silylation of the hydroxy group allows purification of **7** by alumina column
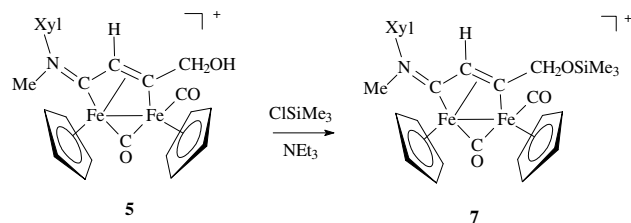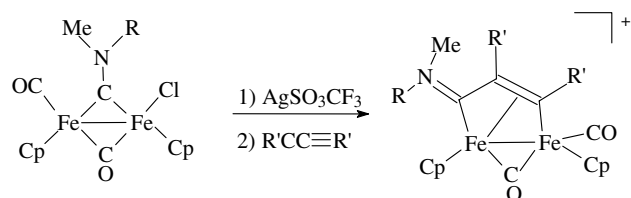

Scheme 4.

chromatography, whereas the parent compound **5** could only be filtered on celite. This reaction could, in principle, be used to anchor **5** on solid silica supports.

2.2. Insertion of symmetrically-disubstituted alkynes

Disubstituted alkynes (2-butyne and 3-hexyne) also insert into the metal carbyne carbon bond of **1a** to form the corresponding complexes [Fe₂{μ-σ:η³-C(R')=C(R')C=N(Me)(Xyl)}(μ-CO)(CO)(Cp)₂][SO₃CF₃] (R' = Me, **8**; Et, **9**); however, better yields are obtained upon treatment of the chloride complexes [Fe₂{μ-CN(Me)(R)}(μ-CO)(CO)(Cl)(Cp)₂] with AgSO₃CF₃ in the presence of the appropriate alkyne (Scheme 5). The ^{1}H NMR data of the green compounds **8** and **9** show some significant differences compared to those of the red-brown complexes obtained from primary alkynes (e.g. the N-bonded methyl and one of the Cp resonances appear up field shifted). In order to establish whether these differences correspond to significant changes in the geometry, the X-ray molecular structure of **8** has been determined. The latter is shown in Fig. 2 and some important configuration novelties are evident: (i) the Cp ligands are mutually *trans* (*trans*-**8**) while they are *cis* in **2** (Fig. 1); (ii) the iminium group –N(Me)(Xyl) is rotated by 180° with respect to **2**, producing a *Z* isomer.

The ^{1}H NMR data of **8** and **9** are in good agreement with the geometry observed in the solid state and shown in Fig. 2. Resonances due to the N–Me protons in **8** and **9** occur at 3.61 and 3.63 ppm, respectively, that is in the range expected for *Z* isomers.

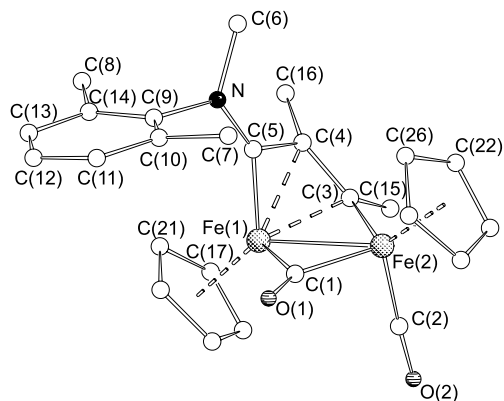|	**R**	**R'**
8	Xyl	Me
9	Xyl	Et
10	Xyl	CO₂Me
11	CH₂Ph	CO₂Me
12	Me	CO₂Me

Scheme 5.

Fig. 2. Molecular structure of the cation of *trans*-[Fe₂{μ-σ:η³-C(Me)=C(Me)C=N(Me)(Xyl)}(μ-CO)(CO)(Cp)₂][SO₃CF₃] (*trans*-**8**). Hydrogen atoms have been omitted for clarity.

Steric factors are likely to be important in favouring *Z* isomers: increasing steric demand at the C$_\beta$ position, due to a methyl (or ethyl) substituent, presumably forces the Xyl group far apart. The mutual *trans*-position adopted by the Cp ligands in **8** is remarkable because most of the related complexes, containing the Fe₂Cp₂(CO)₂ frame and bridging carbon ligands display *cis*-geometry in the solid state, with few exceptions [4c,6].

In order to investigate its stability, *trans*-**8** has been dissolved in THF and heated at refluxing temperature for 60 min. The treatment has resulted in a complete isomerization to *cis*-**8**, as ascertained by an X-ray diffraction study. The structure (Fig. 3) also shows that *E–Z* isomerization has not taken place under these conditions. NMR studies evidence that *cis*-**8** retains the *Z*-configuration also in solution. In particular, the NMe protons resonate at 3.37 ppm, as expected for a *Z*-isomer. Furthermore, the configuration of complex *cis*-**8** in solution has been confirmed by NOE studies, which reveal strong enhancement of the resonance due to the N–Me when the C$_\beta$–Me is irradiated. Thus, the methyl on the nitrogen points towards the C$_\beta$–Me, as expected for a *Z*-isomer and, consequently, the Xyl group points

towards one Cp ligand. Accordingly, NOE is shown between the Xyl group and one Cp ligand.

Additionally, a significant NOE has been detected between the two Cp ligands, as expected from the relative *cis*-geometry. Coherently, analogous investigations carried out on *trans*-**8** have not evidenced any NOE between the cyclopentadienyl rings.

An analysis of corresponding bond distances in *trans*-**8**, *cis*-**8** (Table 2) and **2** (Table 1) shows that the observed different geometries (*E–Z* and *cis–trans*) have no effect on all the relevant bond distances.

The observed isomerization is not surprising, since *cis–trans* interconversions are rather common in the diiron frame Fe₂(μ-CO)(CO)₂(Cp)₂. Adams and Cotton put forward a mechanism for the *cis–trans* isomerization of [Fe₂(μ-CO)₂(CO)₂(Cp)₂] which is now a textbook example of the dynamic behaviour of metal carbonyl compounds [7] and *cis–trans* interconversion has been investigated in other related dinuclear complexes with μ-alkylidenes [8], μ-CNR [9], and μ-vinyl [10].

Analogous behaviour has been observed for [Fe₂{μ-σ:η³-C(Et)=C(Et)C=N(Me)(Xyl)}(μ-CO)(CO)(Cp)₂][SO₃-CF₃] (**9**). Its synthesis from the chloride complex [Fe₂{μ-CN(Me)(Xyl)}(μ-CO)(CO)(Cl)(Cp)₂] affords *trans*-**9**, which in turn isomerises to *cis*-**9** upon heating in THF at reflux.

Since the observed *trans* to *cis* isomerization is temperature dependent, the formation of vinyliminium complexes from chloride precursors, which can be
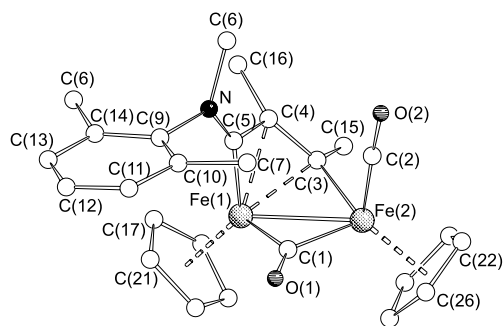

Fig. 3. The molecular structure of the cation of *cis*-[Fe₂{μ-σ:η³-C(Me)=C(Me)C=N(Me)(Xyl)}(μ-CO)(CO)(Cp)₂][SO₃CF₃] (*cis*-**8**). Hydrogen atoms have been omitted for clarity.

Table 2
Selected bond lengths (Å) and angles (°) for *cis*-**8** and *trans*-**8**

	Trans-**8**	*Cis*-**8**
Fe(1)–Fe(2)	2.559(1)	2.562(1)
Fe(1)–C(3)	2.004(6)	2.035(7)
Fe(1)–C(4)	2.096(5)	2.080(7)
Fe(1)–C(5)	1.819(6)	1.839(7)
Fe(1)–C(1)	1.996(6)	1.944(8)
Fe(2)–C(1)	1.874(6)	1.894(8)
C(1)–O(1)	1.167(7)	1.181(9)
Fe(2)–C(3)	1.978(5)	1.955(7)
C(3)–C(4)	1.381(8)	1.39(1)
C(4)–C(5)	1.434(7)	1.43(1)
C(5)–N	1.324(7)	1.314(8)
C(6)–N	1.488(7)	1.478(9)
C(9)–N	1.448(8)	1.454(8)
C(3)–C(15)	1.511(8)	1.54(1)
C(4)–C(16)	1.523(7)	1.52(1)
Fe(2)–C(2)	1.741(8)	1.750(9)
C(2)–O(2)	1.150(8)	1.150(9)
Fe(1)–C(Cp)(av)	2.093	2.090
Fe(2)–C(Cp)(av)	2.119	2.109
C(9)–N–C(5)	120.2(5)	121.9(6)
C(5)–C(4)–C(3)	114.0(5)	115.5(6)
N–C(5)–C(4)	129.6(5)	131.3(7)
Fe(2)–C(3)–C(4)	119.4(4)	121.8(5)
Fe(1)–C(5)–C(4)	79.3(3)	77.9(4)
C(5)–N–C(6)	123.4(5)	121.9(6)
C(6)–N–C(9)	116.3(5)	116.2(5)

performed at room temperature, appears to be the most favourable route for obtaining *trans* isomers. However, it should be noted that the same synthetic method, when applied to primary alkynes, exclusively yields *cis*-isomers. Therefore the formation of *trans*-**8** and *trans*-**9** is strictly related to the nature of disubstituted alkynes: 2-butyne and 3-hexyne.

The reactions of the acetylene dicarboxylate $MeO_2CC\equiv CCO_2Me$ with $[Fe_2\{\mu-CN(Me)(R)\}(\mu-CO)(CO)(Cl)(Cp)_2]$ (R = Xyl, CH$_2$Ph, Me) and AgSO$_3$CF$_3$ have also been investigated. The insertion reactions occur as expected affording the vinyliminium complexes $[Fe_2\{\mu-\sigma:\eta^3-C(CO_2Me)=C(CO_2Me)C=N(Me)(R)\}(\mu-CO)(CO)(Cp)_2][SO_3CF_3]$ (R = Xyl, **10**; R = CH$_2$Ph, **11**; R = Me, **12**) in good yields (Scheme 5). The ^{1}H NMR spectrum of **10** indicates the presence of one single isomer. Comparison of the Cp and NMe resonances (at 5.36, 4.92 and 3.50 ppm, respectively) with those of the complexes *cis*-**8** and *trans*-**8** suggests that **10** adopts *cis* geometry and *Z* orientation. The complete absence of *trans*-**10**, although the synthesis is performed in the same conditions described for **8** and **9**, should be possibly related to the electron-withdrawing character of the COOMe groups, besides their steric demand. The presence of two carboxylate groups in **10** is revealed by the IR ν-CO absorptions at 1733 and 1717 cm^{-1}. Moreover, ^{1}H NMR resonances due to the COOMe are observed at 4.17 and 3.98 ppm, whereas ^{13}C NMR signals at 176.4 and 166.7 ppm are tentatively attributed to the carboxylate carbons bonded to C$_\gamma$ and C$_\beta$, respectively.

Complex $[Fe_2\{\mu-\sigma:\eta^3-C(COOMe)=C(COOMe)C=N(Me)(CH_2Ph)\}(\mu-CO)(CO)(Cp)_2][SO_3CF_3]$ (**11**) exists in solution as a mixture of two isomers, identified, on the basis of their NMR data, as *cis-E* and *cis-Z*, with predominance of the latter. Steric arguments should explain the presence of the *E* isomer, whereas **8**, **9** and **10** are exclusively *Z*. In the latter complexes, the steric demanding Xyl group can assume only one of the two possible orientations, corresponding to the *Z* isomer. By contrast, the lower difference of steric hindrance between Me and CH$_2$Ph in **11**, allow the formation of both isomers (*E* and *Z*) although *Z* still prevails. Finally, only one *cis* isomer is observed in the NMR spectra of $[Fe_2\{\mu-\sigma:\eta^3-C(COOMe)=C(COOMe)C=NMe_2\}(\mu-CO)(CO)(Cp)_2][SO_3CF_3]$ (**12**), because the substituents at the iminium nitrogen are identical. The ^{1}H NMR spectrum of **12** well evidences the different chemical shift of the two N-bonded methyl groups, at 3.81 and 3.22 ppm. These are attributable to the protons pointing toward the Cp and the C$_\beta$(COOMe), respectively.

2.3. Insertion of 2-hexyne

Insertion of an unsymmetrically disubstituted alkyne, like 2-hexyne, into the μ-carbyne–iron bond of **1a**, potentially gives rise to eight different isomers, because of the possible *E–Z*, *cis–trans* geometries and head–head and head–tail insertion modes.

As for the other disubstituted alkynes the insertion of 2-hexyne is better performed on the complex $[Fe_2\{\mu-CN(Me)(R)\}(\mu-CO)(CO)(Cl)(Cp)_2]$ (R = Xyl, Me), treated in situ with AgSO$_3$CF$_3$. The reaction of $[Fe_2\{\mu-CN(Me)(Xyl)\}(\mu-CO)(CO)(Cl)(Cp)_2]$ with 2-hexyne affords a mixture of $[Fe_2\{\mu-\sigma:\eta^3-C(CH_2CH_2CH_3)=C(Me)C=N(Me)(Xyl)\}(\mu-CO)(CO)(Cp)_2][SO_3CF_3]$ (**13**) and $[Fe_2\{\mu-\sigma:\eta^3-C(Me)=C(CH_2CH_2CH_3)C=N(Me)(Xyl)\}(\mu-CO)(CO)(Cp)_2][SO_3CF_3]$ (**14**), both present as *cis* and *trans* isomers (Scheme 6), which could not be separated by chromatography.

The corresponding ^{1}H NMR spectra contain four sets of signals that have been attributed to *trans*-**13**, *trans*-**14**, *cis*-**13** and *cis*-**14** by comparison with the NMR data of *cis*-**8** and *trans*-**8**. The relative amounts of the four isomers are 10:4:3:1, respectively. All the isomeric forms show NMe signals at about 3.6 ppm, indicating that the methyl group points toward the C$_\beta$ (*Z* orientation). The predominant isomers (*trans*-**13** and *trans*-**14**) are the result of the two possible insertion modes of 2-hexyne into the Fe–carbyne bond: *trans*-**13** shows a methyl group on C$_\beta$ and a CH$_2$CH$_2$CH$_3$ group bound to C$_\gamma$; *trans*-**14** exhibits the opposite sequence.

Trans-**13** and *trans*-**14** can be distinguished, in the ^{1}H NMR spectra, because the resonance of C$_\gamma$Me is downfield shifted compared to that of C$_\beta$Me. The insertion of 2-hexyne into the metal–carbyne bond of $[Fe_2\{\mu-CN(Me_2)\}(\mu-CO)(CO)(Cl)(Cp)_2]$ proceeds similarly, affording a mixture of *trans*-**15**, *cis*-**16**, and *cis*-**15**, in 7:5:2 ratio, respectively. Again, the predominant

| R | Xyl | **13** |
| R | Me | **15** |

| R | Xyl | **14** |
| R | Me | **16** |
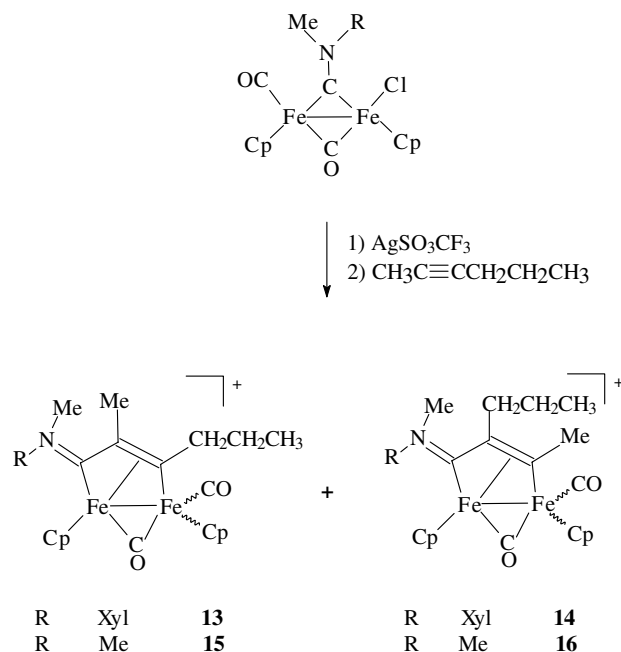
Scheme 6.

isomer displays *trans* geometry, with the Me group bonded to the C_β carbon. In other words, coupling between the μ-carbyne and the alkyne carbons occurs preferentially with the less hindered alkyne carbon.

Treatment of the reaction mixture containing *trans*-**13**, *trans*-**14**, *cis*-**13** and *cis*-**14** in THF at refluxing temperature for 4 h results in complete isomerization of *trans*-**13** and *trans*-**14** to *cis*-**13** and *cis*-**14**, respectively. The relative amounts of **13** and **14** remain unchanged (the ratio is about 13/5) indicating that the *cis* to *trans* isomerization is not accompanied by **13**–**14** interconversion.

The formation of **13** and **14**, as well as **15** and **16**, shows that the insertion of 2-hexyne is not regiospecific, as that of primary alkynes (HC≡CR′). The latter is presumably a consequence of the relevant difference in steric demand between H and R′.

3. Conclusions

Our studies on alkynes insertion into the Fe–carbyne bond have been extended to a number of mono- and disubstituted alkynes with the aim to investigate the nature and geometry of the isomeric species formed. We have found that the stereochemistry of the reaction largely depends on the nature of the alkyne. Insertion of primary alkynes is regiospecific and the products exclusively exhibit *cis*-geometry. Moreover iminium substituents (Me, Xyl) preferentially adopt one of two possible orientations, corresponding to the *E* isomer. By contrast, the insertion of disubstituted alkynes (2-butyne, 3-hexyne, 2-hexyne) yields both *trans* and *cis* isomers. The latter appear more stable and *trans* to *cis* isomerization occurs upon thermal treatment. Insertion of disubstituted alkynes, in place of primary alkynes, results in higher steric hindrance on the C_β position of the vinyl iminium ligand and this has two important consequences: (i) the iminium substituents (Me, Xyl) adopt opposite orientation with respect to that found with primary alkynes and corresponding to the *Z* isomer; (ii) the insertion lose its regiospecific character and both insertion modes (head–head or head–tail) are observed.

However, our findings demonstrate that the insertion of alkynes has a general character and tolerates functional groups, which should expand the reactivity of the bridging vinyliminium ligand that we are investigating.

4. Experimental

4.1. General

Reactions were routinely carried-out under nitrogen using standard Schlenk-line techniques. Solvents were distilled immediately before use under nitrogen from appropriate drying agents. Glassware was oven-dried before use. Infrared spectra were recorded on a Perkin–Elmer 983-G spectrophotometer. All NMR measurements were performed on Varian Gemini 300 and Mercury 400 instruments at room temperature. The chemical shifts for ^{1}H and ^{13}C are referenced to internal TMS. Unless otherwise stated, NMR signals due a second isomeric form (where it has been possible to detect and/or resolve them) are italicized. NOE measurements were recorded using DPFGSE-NOE sequence [11]. All the reagents were commercial products (Aldrich) of the highest purity available and used as received. [Fe₂(CO)₄(Cp)₂] was purchased from Strem and used as received. Compounds [Fe₂{μ-CN(Me)R}(μ-CO)(CO)₂(Cp)₂][SO₃CF₃] (R = 2,6-Me₂C₆H₃, CH₂Ph, Me) [12] and their derivatives [Fe₂{μ-CN(Me)R}(μ-CO)(CO)(NCMe)(Cp)₂][SO₃CF₃], [Fe₂{μ-CN(Me)R}(μ-CO)(CO)(Cl)(Cp)₂] [4b] were prepared as described in the literature.

4.2. Syntheses of [Fe₂{μ-σ:η³-C(CO₂Me)=CHC=N(Me)(R)}(μ-CO)(CO)(Cp)₂][SO₃CF₃] (R = Xyl, **2**; R = CH₂Ph, **3**; R = Me, **4**)

Compound **1a** (90 mg, 0.15 mmol) and HC≡CCO₂Me (0.15 ml, 1.8 mmol), in CH₂Cl₂ solution (10 ml), were heated at refluxing temperature for 4 h. Then, the solvent was removed under reduced pressure; the residue was washed with Et₂O (2 × 10 ml), dissolved in CH₂Cl₂ (10 ml) and filtered through celite. Removal of the solvent in vacuum and a subsequent crystallization at −20 °C from CH₂Cl₂ solution layered with diethyl ether gave brown crystals of **2**. Yield 86 mg (88%). Found: C, 48.01; H, 3.90. C₂₇H₂₆F₃Fe₂NO₇S requires: C, 47.88; H, 3.87%. IR (CH₂Cl₂) *v*(CO) 2013 (vs), 1829 (s), 1712 (m); *v*(CN) 1635 (m) cm⁻¹. ^{1}H NMR (CDCl₃) δ 7.44–6.92 (m, 3H, Me₂C₆*H*₃); 5.35, 5.34, *5.24*, *4.88* (s, 10H, Cp); 4.43 (s, 1H, C$_\beta$H); 4.20, *3.57* (s, 3H, NMe); *4.16*, 4.05 (s, 3H, CO₂Me); *2.59*, 2.29, *1.93*, 1.73 (s, 6H, *Me*₂C₆H₃); (*E*:*Z* ratio = 6). ^{13}C NMR (CDCl₃) δ 250.2 (μ-CO); 230.1 (C$_\alpha$); *209.1*, 208.2 (CO); 186.3 (C$_\gamma$); 177.0 (*CO*₂Me), 144.9 (ipso-Me₂C₆H₃); 131.5–129.2 (Me₂*C₆*H₃); 91.2, *90.9*, 89.2, *88.7* (Cp); 53.3 (CO₂*Me*), 52.2 (C$_\beta$); 46.6 (NMe); 18.1, *17.6*, 17.1 (*Me*₂C₆H₃).

Complex **3** has been obtained following the same procedure described for the synthesis of **2**, by reacting [Fe₂{μ-CN(Me)(CH₂Ph)}(μ-CO)(CO)(NCMe)(Cp)₂][SO₃CF₃] (**1b**; 300 mg, 0.49 mmol) with HC≡CCO₂Me (0.15 ml, 1.8 mmol). Yield 216 mg (66%). Found: C, 47.08; H, 3.77. C₂₆H₂₄F₃Fe₂NO₇S requires: C, 47.09; H, 3.65%. IR (CH₂Cl₂) *v*(CO) 2000 (vs), 1817 (s), 1710 (m); *v*(CN) 1671 (m) cm⁻¹. ^{1}H NMR (CDCl₃) δ 7.40–7.06 (m, 5H, C₆*H*₅); *5.58*, *5.40*, 5.05, 4.58 (d, $^2J_{HH}$ = 14 Hz, C*H*₂Ph); *5.25*, 5.13 (s, 1H, C$_\beta$H); *5.23*, 5.21, *5.19* (s, 10H, Cp); 4.10, *4.09* (s, 3H, CO₂Me); 3.68, *3.09* (s, 3H, NMe);

(*E:Z* ratio = 1.2). ^{13}C NMR (CDCl$_3$) δ 254.5, *252.7* (μ-CO); *223.7*, 223.1 (C$_\alpha$); *208.6*, 208.4 (CO); 184.1, *183.9* (C$_\gamma$); 177.3 (*CO$_2$*Me); 132.8–129.1 (C$_6$H$_5$); *90.5*, 90.4, 88.8, *88.8* (Cp); *68.4*, 62.0 (CH$_2$Ph); *53.6*, 53.1 (CO$_2$Me); 51.9, *51.5* (C$_\beta$); 48.3, *42.4* (NMe).

Complex **4** has been obtained following the same procedure described for the synthesis of **2**, by reacting [Fe$_2$\{μ-CN(Me)$_2$\}(μ-CO)(CO)(NCMe)(Cp)$_2$][SO$_3$CF$_3$] (**1c**; 85 mg, 0.16 mmol) with HC≡CCO$_2$Me (0.10 ml, 1.2 mmol). Yield: 72 mg (77%). Found: C, 40.84; H, 3.43. C$_{20}$H$_{20}$F$_3$Fe$_2$NO$_7$S requires: C, 40.91; H, 3.43%. IR (CH$_2$Cl$_2$) v(CO) 2000 (vs), 1817 (s), 1710 (m); v(CN) 1687 (m) cm^{-1}. ^{1}H NMR (CD$_2$Cl$_2$) δ 5.15, 5.10 (s, 10H, Cp); 4.94 (s, 1H, C$_\beta$H); 4.03 (s, 3H, CO$_2$Me); 3.78, 3.23 (s, 6H, NMe). ^{13}C NMR (CD$_2$Cl$_2$) 253.1 (μ-CO); 223.1 (C$_\alpha$); 208.6 (CO); 183.2 (C$_\gamma$); 177.2 (*CO$_2$*Me); 90.3, 88.5 (Cp); 53.1, 45.1 (NMe); 51.9 (C$_\beta$); 51.7 (CO$_2$Me).

4.3. Syntheses of [Fe$_2$\{μ-σ:η^3-C(CH$_2$OH)=CHC=N(Me)(R)\}(μ-CO)(CO)(Cp)$_2$][SO$_3$CF$_3$] (R = Xyl, 5; R = Me, 6)

To a solution of **1a** (200 mg, 0.32 mmol), in CH$_2$Cl$_2$ (15 ml), HC≡CCH$_2$OH (0.20 ml, 3.4 mmol) was added and the solution was heated at refluxing temperature for 4 h. Then, the solvent was removed under reduced pressure. The residue was washed with Et$_2$O (2 × 10 ml), dissolved in CH$_2$Cl$_2$ (10 ml) and filtered through celite. Removal of the solvent in vacuum afforded **5** as a dark-brown microcrystalline powder. Yield 169 mg (83%). Found C, 48.17; H, 4.09. C$_{26}$H$_{26}$F$_3$Fe$_2$NO$_6$S requires: C, 48.10; H, 4.04%. IR (CH$_2$Cl$_2$) v(CO) 2001 (vs), 1810 (s); v(CN) 1631 (m) cm^{-1}. ^{1}H NMR (CDCl$_3$) δ 7.34–6.84 (m, 3H, Me$_2$C$_6$H$_3$); 6.31 (dd, 1H, $^2J_{HH}$ = 17 Hz, $^3J_{HH}$ = 6 Hz, CH$_2$OH); 5.65 (dd, 1H, $^2J_{HH}$ = 17 Hz, $^3J_{HH}$ = 5 Hz, CH$_2$OH); 5.35, *5.29*, 5.17, *4.74* (s, 10H, Cp); 5.20 (m, 1H, OH); 4.96 (s, 1H, C$_\beta$H); 4.14, *3.48* (s, 3H, NMe); *2.44*, 2.24, *1.97*, 1.74 (s, 6H, Me$_2$C$_6$H$_3$); (*E:Z* ratio = 5). ^{13}C NMR (CDCl$_3$) δ 254.7, *253.9* (μ-CO); 233.4, *230.9* (C$_\alpha$); 213.3, *212.4* (CO); *210.2*, 209.5 (C$_\gamma$); 144.6, *140.8* (ipso-Me$_2$C$_6$H$_3$); 133.6–128.6 (Me$_2$C$_6$H$_3$); 89.8, 87.4, *87.1* (Cp); 75.2, *71.6* (CH$_2$OH); 51.8 (C$_\beta$); 45.8 (NMe); 17.7, *17.5*, 17.0 (Me$_2$C$_6$H$_3$).

Complex **6** has been obtained following the same procedure described for the synthesis of **5**, by reacting **1c** (120 mg, 0.23 mmol) with HC≡CCH$_2$OH (0.10 ml, 1.7 mmol). Yield 104 mg (82%). Found: C, 40.80; H, 3.64. C$_{19}$H$_{20}$F$_3$Fe$_2$NO$_6$S requires: C, 40.82; H, 3.61%. IR (CH$_2$Cl$_2$) v(CO) 1991 (vs), 1806 (s); v(CN) 1681 (m) cm^{-1}. ^{1}H NMR (CDCl$_3$) δ 6.16, 5.88 (dd, 2H, $^2J_{HH}$ = 15 Hz, $^3J_{HH}$ = 3 Hz, CH$_2$OH); 5.25 (s, 1H, C$_\beta$H); 5.22, 5.02 (s, 10H, Cp); 5.00 (t, 1H, $^3J_{HH}$ = 3 Hz, OH); 3.80, 3.25 (s, 6H, NMe). ^{13}C NMR (CDCl$_3$) δ 257.0 (μ-CO); 226.1 (C$_\alpha$); 210.0, 209.5 (CO and C$_\gamma$); 89.0, 87.3 (Cp); 75.2 (CH$_2$OH); 50.9, 44.8 (NMe); 46.5 (C$_\beta$).

4.4. Synthesis of [Fe$_2$\{μ-σ:η^3-C(CH$_2$OSiMe$_3$)=CHC=N(Me)(Xyl)\}(μ-CO)(CO)(Cp)$_2$][SO$_3$CF$_3$] (7)

A CH$_2$Cl$_2$ solution (10 ml) of complex **6** (71 mg, 0.109 mmol) was treated with Me$_3$SiCl (0.5 ml, 3.9 mmol) and Et$_3$N (15 mmol) at refluxing temperature for 5 h. Solvent removal and chromatography of the residue on alumina column eluting with CH$_2$Cl$_2$, first, and with CH$_3$CN, then, gave a yellow-brown fraction. Crystallization from CH$_2$Cl$_2$–Et$_2$O solution afforded **7**. Yield 47 mg (60%). Found: C, 48.19; H, 4.77. C$_{29}$H$_{34}$F$_3$Fe$_2$NO$_6$SSi requires: C, 48.28; H, 4.75%. IR (CH$_2$Cl$_2$) v(CO) 1999 (vs), 1817 (s); v(CN) 1632 (m) cm^{-1}. ^{1}H NMR (CDCl$_3$) δ 7.50–6.92 (m, 3H, Me$_2$C$_6$H$_3$); 6.05, 5.96 (d, 2H, $^3J_{HH}$ = 15.6 Hz, CH$_2$OSi); 5.39, 5.10 (s, 10H, Cp); 4.74 (s, 1H, C$_\beta$H); 4.17 (s, 3H, NMe); 2.22, 1.76 (s, 6H, Me$_2$C$_6$H$_3$); 0.21 (s, 9H, SiMe$_3$). ^{13}C NMR (CDCl$_3$) δ 254.0 (μ-CO); 233.2 (C$_\alpha$); 210.2, 209.6 (CO and C$_\gamma$); 144.9–122.7 (Me$_2$C$_6$H$_3$); 89.9, 87.6 (Cp); 75.6 (CH$_2$O); 51.9 (NMe); 49.0 (C$_\beta$); 17.7, 17.2 (Me$_2$C$_6$H$_3$); 1.01 (SiMe$_3$). ESI-MS: ES$^+$ 572.

4.5. Synthesis of trans and cis isomers of [Fe$_2$\{μ-σ:η^3-C(Me)=C(Me)C=N(Me)(Xyl)\}(μ-CO)(CO)(Cp)$_2$][SO$_3$CF$_3$] (8)

To a solution of [Fe$_2$\{μ-CN(Me)(Xyl)\}(μ-CO)(CO)(Cl)(Cp)$_2$] (232 mg, 0.48 mmol), in CH$_2$Cl$_2$ (15 ml), cooled at −20 °C, MeC≡CMe (0.30 ml, 3.8 mmol) and AgSO$_3$CF$_3$ (174 mg, 0.68 mmol) were added. The mixture was stirred for about 15 min. Removal of the solvent and then chromatography on an alumina column, with a mixture of MeCN:THF (1:1, v:v) as eluent, gave a green band which was collected. Crystallization from CH$_2$Cl$_2$ layered with Et$_2$O afforded green crystals of *trans*-**8**. Yield 188 mg (60%). Found: C, 50.16; H, 4.39. C$_{27}$H$_{28}$F$_3$Fe$_2$NO$_5$S requires: C, 50.10; H, 4.36%. IR (CH$_2$Cl$_2$) v(CO) 1986 (vs), 1826 (s); v(CN) 1608 (w) cm^{-1}. ^{1}H NMR (CDCl$_3$) δ 7.48–6.91 (m, 3H, Me$_2$C$_6$H$_3$); 4.73, 4.47 (s, 10H, Cp); 3.91 (s, 3H, C$_\gamma$Me); 3.61 (s, 3H, NMe); 2.48, 2.08 (s, 6H, Me$_2$C$_6$H$_3$); 2.15 (s, 3H, C$_\beta$Me). ^{13}C NMR (CDCl$_3$) δ 251.4 (μ-CO); 230.0 (C$_\alpha$); 208.8 (CO); 204.4 (C$_\gamma$); 141.8 (ipso-Me$_2$C$_6$H$_3$); 133.9–128.9 (Me$_2$C$_6$H$_3$); 89.4, 88.4 (Cp); 69.4 (C$_\beta$); 49.9 (NMe); 37.9 (Cγ Me); 18.1, 17.8 (Me$_2$C$_6$H$_3$); 16.5 (C$_\beta$Me).

A solution of *trans*-**8** (188 mg, 0.29 mmol) in THF (15 ml) was heated at refluxing temperature for 60 min. Crystallization from CH$_2$Cl$_2$ solution layered with Et$_2$O afforded red crystals of *cis*-**8**. Yield 156 mg (83%). Found: C, 50.13; H, 4.35. C$_{27}$H$_{28}$F$_3$Fe$_2$NO$_5$S requires: C, 50.10; H, 4.36%. IR (CH$_2$Cl$_2$) v(CO) 1986 (vs), 1818 (s); v(CN) 1613 (w) cm^{-1}. ^{1}H NMR (CDCl$_3$) δ 7.48–7.00 (m, 3H, Me$_2$C$_6$H$_3$); 5.29, 4.68 (s, 10H, Cp); 3.88, (s, 3H, C$_\gamma$Me); 3.37 (s, 3H, NMe); 2.49, 1.99 (s, 6H, Me$_2$C$_6$H$_3$); 2.10 (s, 3H, C$_\beta$Me). ^{13}C NMR (CDCl$_3$) δ 254.2 (μ-CO);

230.7 (C_α); 210.8 (CO); 204.6 (C_γ); 140.4 (ipso-$Me_2C_6H_3$); 134.1–128.9 ($Me_2C_6H_3$); 91.3, 88.1 (Cp); 65.7 (C_β); 50.1 (NMe); 37.7 ($C\gamma Me$); 17.9 ($Me_2C_6H_3$); 16.6 ($C_\beta Me$).

4.6. Synthesis of trans and cis isomers of $Fe_2\{\mu\text{-}\sigma:\eta^3\text{-}C(Et)=C(Et)C=N(Me)(Xyl)\}(\mu\text{-}CO)(CO)(Cp)_2]$ $[SO_3CF_3]$ (9)

Complex *trans*-**9** was obtained with the same procedure described for *trans*-**8**, using [Fe$_2$\{μ-CN(Me)(Xyl)\}(μ-CO)(CO)(Cl)(Cp$_2$)] (123 mg, 0.26 mmol), CH$_3$CH$_2$C≡CCH$_2$CH$_3$ (0.20 ml, 1.8 mmol), and AgSO$_3$CF$_3$ (99 mg, 0.39 mmol). Yield 116 mg (66%). Found: C, 51.68; H, 4.80%. C$_{29}$H$_{32}$F$_3$Fe$_2$NO$_5$S requires: C, 51.58; H, 4.78%. IR (CH$_2$Cl$_2$) v(CO) 1986 (vs), 1828 (s); v(CN) 1605 (w) cm^{-1}. ^{1}H NMR (CDCl$_3$) δ 7.48–7.23 (m, 3H, $Me_2C_6H_3$); 4.73, 4.49 (s, 10H, Cp); 4.24, 4.11 (m, 2H, C_γ-CH_2); 3.63 (s, 3H, NMe); 2.80, 1.84 (m, 2H, C_β-CH_2); 2.50, 2.13 (s, 6H, $Me_2C_6H_3$); 1.85 (t, $^3J_{HH} = 7$ Hz, 3H, C_γ-CH$_2$CH_3); 1.63 (t, $^3J_{HH} = 7$ Hz, 3H, C_β-CH$_2$CH_3). ^{13}C NMR (CDCl$_3$) δ 251.7 (μ-CO); 230.0 (C_α); 213.1 (C_γ); 209.2 (CO); 140.5–129.0 ($Me_2C_6H_3$); 89.4, 89.0 (Cp); 67.9 (C_β); 51.1 (NMe); 43.4 (C_γ-CH$_2$); 26.0 (C_β-CH$_2$); 20.0 (C_γ-CH$_2$CH$_3$); 18.4 ($Me_2C_6H_3$); 14.9 (C_β-CH$_2$CH$_3$).

Cis-**9** was obtained as described for *cis*-**8**, by heating a THF solution of *trans*-**9** (116 mg, 0.17 mmol). Yield 65 mg (56%). Found: C, 51.66; H, 4.79. C$_{29}$H$_{32}$F$_3$Fe$_2$NO$_5$S requires: C, 51.58; H, 4.78%. IR (CH$_2$Cl$_2$) v(CO) 1984 (vs), 1817 (s); v(CN) 1613 (w) cm^{-1}. ^{1}H NMR (CDCl$_3$) δ 7.45–7.23 (m, 3H, $Me_2C_6H_3$); 5.30, 4.69 (s, 10H, Cp); 4.24, 4.11 (m, 2H, C_γ-CH_2); 3.40 (s, 3H, NMe); 2.80, 1.84 (m, 2H, C_β-CH_2); 2.51, 1.97 (s, 6H, $Me_2C_6H_3$); 1.80 (t, $^3J_{HH} = 7$ Hz, 3H, C_γ-CH$_2$CH_3); 1.54 (t, $^3J_{HH} = 7$ Hz, 3H, C_β-CH$_2$CH_3). ^{13}C NMR (CDCl$_3$) δ 253.9 (μ-CO); 230.6 (C_α); 214.0 (C_γ); 211.0 (CO); 140.3 (ipso-$Me_2C_6H_3$); 134.0, 133.3, 129.8, 129.7, 128.9 ($Me_2C_6H_3$); 90.9, 88.0 (Cp); 68.1 (C_β); 51.2 (NMe); 42.8 (C_γ-CH$_2$); 25.7 (C_β-CH$_2$); 20.7 (C_γ-CH$_2C$H$_3$); 18.2 ($Me_2C_6H_3$); 15.5 (C_β-CH$_2$CH$_3$).

4.7. Syntheses of $[Fe_2\{\mu\text{-}\sigma:\eta^3\text{-}C(CO_2Me)=C(CO_2Me)C=N(Me)(R)\}(\mu\text{-}CO)(CO)(Cp)_2][SO_3CF_3]$ (R=Xyl, 10; R=Bz, 11; R=Me, 12)

A solution of [Fe$_2$\{μ-CN(Me)(Xyl)\}(μ-CO)(CO)(Cl)(Cp)$_2$] (38 mg, 0.079 mmol), in CH$_2$Cl$_2$ (10 ml), was treated with CO$_2$MeC≡CCO$_2$Me (0.10 ml, 0.81 mmol), and then with AgSO$_3$CF$_3$ (25 mg, 0.098 mmol). The mixture was stirred for 10 min, and the solvent was removed; the residue was washed with Et$_2$O (2 × 10 ml), dissolved in CH$_2$Cl$_2$ (10 ml) and filtered through celite. Removal of the solvent in vacuum afforded **10** as orange powder. Yield 51 mg (88%). Found: C, 47.32; H, 3.83. C$_{29}$H$_{28}$F$_3$Fe$_2$NO$_9$S requires: C, 47.37; H, 3.84%. IR

(CH$_2$Cl$_2$) v(CO) 2007 (vs), 1843 (s), 1733 (m), 1717 (m); v(CN) 1629 (mw) cm^{-1}. ^{1}H NMR (CDCl$_3$) δ 7.48–7.20 (m, 3H, $Me_2C_6H_3$); 5.36, 4.92 (s, 10H, Cp); 4.17, 3.98 (s, 6H, CO$_2$Me); 3.50 (s, 3H, NMe); 2.56, 1.97 (s, 6H, $Me_2C_6H_3$). ^{13}C NMR (CDCl$_3$) δ 245.6 (μ-CO); 224.2 (C_α); 208.5 (CO); 190.1 (C_γ); 176.4 (C_γ-CO$_2$Me); 166.7 (C_β-CO$_2$Me); 140.3 (ipso-$Me_2C_6H_3$); 133.6, 133.5, 130.2, 129.9, 129.4 ($Me_2C_6H_3$); 92.2, 89.7 (Cp); 54.0, 53.1 (CO$_2$Me); 53.0 (NMe); 52.1 (C_β); 18.1, 17.4 ($Me_2C_6H_3$).

Complex **11** has been obtained following the same procedure described for the synthesis of **10**, by reacting [Fe$_2$\{μ-CN(Me)(CH$_2$Ph)\}(μ-CO)(CO)(Cl)(Cp)$_2$] (308 mg, 0.66 mmol), in CH$_2$Cl$_2$ (15 ml), with CO$_2$MeC≡CCO$_2$Me (0.30 ml, 2.4 mmol) and AgSO$_3$CF$_3$ (238 mg, 0.93 mmol). Yield 353 mg (74%). Found: 46.59; H, 3.58. C$_{28}$H$_{26}$F$_3$Fe$_2$NO$_9$S requires: C, 46.63; H, 3.63%. IR (CH$_2$Cl$_2$) v(CO) 2008 (vs), 1829 (s), 1733 (s), 1715 (s); v(CN) 1669 (m) cm^{-1}. ^{1}H NMR (CDCl$_3$) δ 7.51–7.12 (m, 5H, Ph); 5.76, 5.43, *5.01, 4.39* (d, 2H, $^2J_{HH} = 15$ Hz, CH_2Ph); 5.32, *5.28, 5.26*, 5.21 (s, 10H, Cp); 4.14, 3.91, *3.86* (s, 6H, CO$_2$Me); *3.77*, 3.05 (s, 3H, NMe); (*E:Z* ratio = 0.5). ^{13}C NMR (CDCl$_3$) δ 250.5, *249.3* (μ-CO); *220.6*, 219.9 (C_α); *207.9*, 207.4 (CO); 188.9 (C_γ); 176.2 (C_γ-CO$_2$Me); 166.5 (C_β-CO$_2$Me); 131.6–128.5 (Ph); *91.6*, 91.5, 89.8, *89.6* (Cp); *68.4*, 62.1 (CH$_2$Ph); 53.7, *53.6*, 52.9 (CO$_2$Me); *51.8*, 51.1 (C_β); 48.5, *42.8* (NMe).

Complex **12** has been obtained following the same procedure described for the synthesis of **10**, by reacting [Fe$_2$\{μ-CN(Me)$_2$\}(μ-CO)(CO)(Cl)(Cp)$_2$] (140 mg, 0.360 mmol) in CH$_2$Cl$_2$ (15 ml), with CO$_2$MeC≡CCO$_2$Me (0.40 ml, 3.2 mmol) and AgSO$_3$CF$_3$ (115 mg, 0.447 mmol). Yield 199 mg (86%). Found: 40.90; H, 3.46. C$_{22}$H$_{22}$F$_3$Fe$_2$NO$_9$S requires: C, 40.96; H, 3.44%. IR (CH$_2$Cl$_2$) v(CO) 2007 (vs), 1830 (s), 1733 (s), 1715 (s); v(CN) 1685 (m) cm^{-1}. ^{1}H NMR (CD$_2$Cl$_2$) δ 5.23, 5.12 (s, 10H, Cp); 4.06, 3.91 (s, 6H, CO$_2$Me); 3.81, 3.22 (s, 6H, NMe). ^{13}C NMR (CD$_2$Cl$_2$) δ 250.1 (μ-CO); 219.7 (C_α); 208.2 (CO); 188.9 (C_γ); 177.1 (C_γ-CO$_2$Me); 166.9 (C_β-CO$_2$Me); 92.3, 90.3 (Cp); 53.7, 52.6 (CO$_2$Me); 52.1 (C_β); 54.6, 46.9 (NMe).

4.8. Syntheses of $[Fe_2\{\mu\text{-}\sigma:\eta^3\text{-}C(CH_2CH_2CH_3)=C(Me)C=N(Me)(R)\}(\mu\text{-}CO)(CO)(Cp)_2][SO_3CF_3]$ (R=Xyl, 13; R=Me, 15) and $[Fe_2\{\mu\text{-}\sigma:\eta^3\text{-}C(Me)=C(CH_2CH_2CH_3)C=N(Me)(R)\}(\mu\text{-}CO)(CO)(Cp)_2][SO_3CF_3]$ (R=Xyl, 14; R=Me, 16)

A solution of [Fe$_2$\{μ-CN(Me)(Xyl)\}(μ-CO)(CO)(Cl)(Cp)$_2$] (156 mg, 0.33 mmol) and 2-hexyne (0.25 ml, 2.2 mmol), in CH$_2$Cl$_2$ (10 ml), was treated with AgSO$_3$CF$_3$ (100 mg, 0.39 mmol). The mixture was stirred for about 15 min. Removal of the solvent and chromatography on an alumina column, using MeOH as eluent, afforded a green band, corresponding to a

mixture of *trans*-**13**, *trans*-**14**, *cis*-**13**, *cis*-**14** (isomer ratio: 10:4:3:1). Yield: 108 mg (49%). Found: C, 51.63; H, 4.81. $C_{29}H_{32}F_3Fe_2NO_5S$ requires: C, 51.58; H, 4.78%. The solid (100 mg) was dissolved in THF and heated at refluxing temperature for 4 hours. Filtration on a celite pad and removal of the solvent afforded a red solid residue consisting of a mixture of *cis*-**13** and *cis*-**14** (84 mg, 84%).

Trans-**13**: IR (CH_2Cl_2): ν(CO) 1986 (vs), 1826 (s); ν(CN) 1607 (m) cm^{-1}. ^{1}H NMR (CDCl$_3$) δ 7.48–7.18 (m, 3H, Me$_2$C$_6$H$_3$); 4.77, 4.45 (s, 10H, Cp); 4.09 (t, 2H, $^3J_{HH} = 8$ Hz, C$_\gamma$-CH_2); 3.62 (s, 3H, NMe); 2.47, 2.13, 2.11 (s, 9H, Me_2C$_6$H$_3$ and C$_\beta$Me); 2.21 (m, 2H, C$_\gamma$-CH$_2$CH_2); 1.34 (t, 3H, $^3J_{HH} = 7$ Hz, C$_\gamma$-CH$_2$CH$_2$CH_3). ^{13}C NMR (CDCl$_3$) δ 252.2 (μ-CO); 229.8 (C$_\alpha$); 209.2, 209.1 (C$_\gamma$ and CO); 141.9 (ipso-Me$_2$C$_6$H$_3$); 134.1–128.7 (Me$_2$C$_6$H$_3$); 88.9, 88.7, (Cp); 70.6 (C$_\beta$); 54.8 (C$_\gamma$-CH$_2$); 49.8 (NMe); 26.4 (C$_\gamma$-CH$_2$CH$_2$); 22.3 (C$_\beta$-CH$_2$CH$_2$); 18.1, 17.9 (Me$_2$C$_6$H$_3$); 15.9, 15.0 (C$_\gamma$-CH$_2$CH$_2$CH$_3$ and C$_\beta$Me).

Trans-**14**: IR (CH_2Cl_2): ν(CO) 1986 (vs), 1826 (s); ν(CN) 1607 (m) cm^{-1}. ^{1}H NMR (CDCl$_3$) δ 7.48–7.18 (m, 3H, Me$_2$C$_6$H$_3$); 4.65, 4.48 (s, 10H, Cp); 3.96 (s, 3H, C$_\gamma$Me); 3.58 (s, 3H, NMe); 2.70, 1.66 (dt, 2H, $^2J_{HH} = 4$ Hz, $^3J_{HH} = 12$ Hz, C$_\beta$-CH_2); 2.49, 2.10 (s, 6H, Me_2C$_6$H$_3$); 1.95 (m, 2H, C$_\beta$-CH$_2$CH_2); 1.19 (t, 3H, $^3J_{HH} = 7$ Hz, C$_\beta$-CH$_2$CH$_2$CH_3). ^{13}C NMR (CDCl$_3$) δ 254.1 (μ-CO); 230.1 (C$_\alpha$); 210.7, 210.4 (C$_\gamma$ and CO); 140.3

(ipso-Me$_2$C$_6$H$_3$); 134.1–128.7 (Me$_2$C$_6$H$_3$); 89.5, 88.6 (Cp); 71.4 (C$_\beta$); 50.5 (NMe); 37.9 (C$_\gamma$Me); 34.2 (C$_\beta$-CH$_2$); 22.3 (C$_\beta$-CH$_2$CH$_2$); 18.6, 17.8 (Me_2C$_6$H$_3$); 14.9 (C$_\beta$-CH$_2$CH$_2$CH$_3$).

Cis-**13**: IR (CH_2Cl_2): ν(CO) 1986 (vs), 1819 (s); ν(CN) 1614 (m) cm^{-1}. ^{1}H NMR (CDCl$_3$) δ 7.48–7.03 (m, 3H, Me$_2$C$_6$H$_3$); 5.28, 4.70 (s, 10H, Cp); 4.13, 4.01 (m, 2H, C$_\gamma$-CH_2); 3.37 (s, 3H, NMe); 2.50, 1.97 (s, 6H, Me_2C$_6$H$_3$); 2.09 (s, 3H, C$_\beta$Me); 1.36 (t, 3H, $^3J_{HH} = 7$ Hz, C$_\gamma$-CH$_2$CH$_2$CH_3). ^{13}C NMR (CDCl$_3$) δ 253.8 (μ-CO); 229.9 (C$_\alpha$); 210.6, 210.1 (C$_\gamma$ and CO); 140.2 (ipso-Me$_2$C$_6$H$_3$); 134.0–128.9 (Me$_2$C$_6$H$_3$); 90.9, 87.9 (Cp); 72.0 (C$_\beta$); 52.9 (C$_\gamma$-CH$_2$); 50.1 (NMe); 27.1 (C$_\gamma$-CH$_2$CH$_2$); 18.0 (Me_2C$_6$H$_3$); 15.8, 14.7 (C$_\gamma$-CH$_2$CH$_2$CH$_3$ and C$_\beta$Me).

Cis-**14**: ^{1}H NMR (CDCl$_3$) δ 7.48–7.03 (m, 3H, Me$_2$C$_6$H$_3$); 5.30, 4.68 (s, 10H, Cp); 3.95 (s, 3H, C$_\gamma$Me); 3.37 (s, 3H, NMe); 2.49, 1.98 (s, 6H, Me_2C$_6$H$_3$); 1.17 (t, 3H, $^3J_{HH} = 7$ Hz, C$_\gamma$-CH$_2$CH$_2$CH_3). ^{13}C NMR (CDCl$_3$) δ 210.8, 219.9 (C$_\gamma$ and CO); 140.6–128.9 (Me$_2$C$_6$H$_3$); 91.2, 88.0 (Cp); 50.4 (NMe); 37.9 (C$_\gamma$-Me); 18.7, 18.3 (Me_2C$_6$H$_3$); 34.3, 22.9, 14.9 (C$_\beta$-CH$_2$CH$_2$CH$_3$).

Complexes **15** and **16** have been obtained following the same procedure described for the synthesis of **13** and **14**, by reacting [Fe$_2$\{μ-CN(Me)$_2$\} μ-CO)(CO)(Cl)(Cp)$_2$] (63 mg, 0.16 mmol) with CH$_3$CH$_2$CH$_2$C≡CCH$_3$ (0.20 ml, 1.8 mmol) and AgSO$_3$CF$_3$ (58 mg, 0.23 mmol), in CH$_2$Cl$_2$ (10 ml). Isomers ratio: *trans*-**15**:*cis*-**16**:*cis*-**15** = 7:5:2; yield: 80 mg, 85%. Found: C, 45.07; H, 4.45.

Table 3
Crystal data and experimental details for **2**, *cis*-**8** and *trans*-**8**

Compound	**2**	*trans*-**8**	*cis*-**8**
Empirical formula	$C_{27}H_{26}F_3Fe_2NO_7S$	$C_{27}H_{28}F_3Fe_2NO_5S$	$C_{27}H_{28}F_3Fe_2NO_5S$
M_r	677.25	647.26	647.26
T/K	293(2)	298(2)	298(2)
λ/Å	0.71073	0.71073	0.71073
Crystal system	Triclinic	Monoclinic	Triclinic
Space group	$P\bar{1}$	$P2_1/c$	$P\bar{1}$
a/Å	10.384(1)	9.0478(4)	8.414(1)
b/Å	11.077(1)	15.4678(7)	12.312(2)
c/Å	12.564(1)	19.4960(9)	14.510(2)
α/°	83.353(3)	90	64.895(3)
β/°	85.939(3)	92.029(2)	82.814(4)
γ/°	77.068(3)	90	85.130(4)
V/Å^3	1397.6(3)	2726.7(2)	1349.5(3)
Z	2	4	2
D_c/Mg m^{-3}	1.609	1.577	1.593
μ (Mo K$_\alpha$)/mm^{-1}	1.179	1.199	1.212
F (0 0 0)	692	1328	664
Crystal size/mm	0.27 × 0.13 × 0.10	0.30 × 0.27 × 0.20	0.30 × 0.24 × 0.20
θ limits/°	2.53–23.99	2.61–24.99	1.56–23.27
Reflections collected	8336($\pm h, \pm k, \pm l$)	24727($\pm h, \pm k, \pm l$)	9993($\pm h, \pm k, \pm l$)
Unique observed reflections [$I > 2\sigma(I)$]	4302 [$R_{int} = 0.074$]	4796 [$R_{int} = 0.090$]	3859 [$R_{int} = 0.072$]
Goodness-of-fit-on F^2	1.069	1.020	0.940
Final R_1[a], $wR_2(F^2)$[b][$I > 2\sigma(I)$]	0.0647, 0.1394	0.0652, 0.1694	0.0611, 0.1512
Largest diff. peak and hole/e Å^{-3}	0.723 and −0.612	0.532 and −0.694	0.618 and −0.580

[a] $R_1 = \sum ||F_o| - |F_c|| / \sum |F_o|$.

[b] $wR_2 = \left[\sum w(F_o^2 - F_c^2)^2 / \sum w(F_o^2)^2 \right]^{1/2}$, where $w = 1/[\sigma^2(F_o^2) + (aP)^2 + bP]$, where $P = (F_o^2 + 2F_c^2)/3$.

$C_{22}H_{26}F_3Fe_2NO_5S$ requires: C, 45.15; H, 4.48%. IR (CH_2Cl_2) ν(CO) 1984 (vs), 1812 (s); ν(CN) 1673 (m) cm^{-1}.

Trans-**15**: ^{1}H NMR (CDCl$_3$) δ 4.78, 4.51 (s, 10H, Cp); 3.94 (t, 2H, $^3J_{HH} = 9$ Hz, C$_\gamma$-CH$_2$); 3.85, 3.32 (s, 6H, NMe); 2.03 (m, 2H, C$_\gamma$-CH$_2$CH$_2$); 1.92 (s, 3H, C$_\beta$Me); 1.28 (t, 3H, $^3J_{HH} = 7$ Hz, 3H, C$_\gamma$-CH$_2$CH$_2$CH$_3$). ^{13}C NMR (CDCl$_3$) δ 255.1 (μ-CO); 225.7 (C$_\alpha$); 210.1 (CO); 201.9 (C$_\gamma$); 90.4, 87.9 (Cp); 68.5 (C$_\beta$); 52.4 (C$_\gamma$-CH$_2$); 49.5, 45.4 (NMe); 32.8 (C$_\gamma$-CH$_2$CH$_2$); 14.7, 14.6 (C$_\gamma$-CH$_2$CH$_2$CH$_3$ and C$_\beta$Me).

Cis-**16**: ^{1}H NMR (CDCl$_3$) δ 5.17, 4.89 (s, 10H, Cp); 3.91, 3.80, 3.14 (s, 9H, NMe and Cγ Me); 2.37, 1.73 (dt, 2H, $^2J_{HH} = 4$ Hz, $^3J_{HH} = 13$ Hz, C$_\beta$-CH$_2$); 1.49 (m, 2H, C$_\beta$-CH$_2$CH$_2$); 1.04 (t, 3H, $^3J_{HH} = 7$ Hz, 3H, C$_\beta$-CH$_2$CH$_2$CH$_3$). ^{13}C NMR (CDCl$_3$) δ 257.7 (μ-CO); 222.3 (C$_\alpha$); 209.3 (CO); 202.5 (C$_\gamma$); 88.9, 88.5 (Cp); 69.2 (C$_\beta$); 48.2, 45.4 (NMe); 37.1 (C$_\gamma$Me); 27.0 (C$_\beta$-CH$_2$); 22.8 (C$_\beta$-CH$_2$CH$_2$); 14.6 (C$_\beta$-CH$_2$CH$_2$CH$_3$).

Cis-**15**: ^{1}H NMR (CDCl$_3$) δ 5.18, 4.95 (s, 10H, Cp); 3.86, 3.15 (s, 6H, NMe); 1.89 (s, 3H, C$_\beta$Me).

4.9. Crystallography

The X-ray intensity data for **2**, *cis*-**8** and *trans*-**8** were measured on a Bruker AXS SMART 2000 diffractometer, equipped with a CCD detector. For all crystals, a full sphere of reciprocal space was scanned by 0.3° ω steps, with the detector kept at 5.0 cm from the sample. Intensity control was monitored by recollecting the initial 50 frames at the end of the data collection and analyzing the duplicate reflections. The software SMART [13] was used for collecting frames of data, indexing reflections and determination of lattice parameters. The collected frames were then processed for integration by the SAINT program [13] and an empirical absorption correction was applied using SADABS [14]. The structures were solved by direct methods (SIR 97) [15] and subsequent Fourier syntheses and refined by full-matrix least-squares on F^2 (SHELXTL) [16], using anisotropic thermal parameters for all non-hydrogen atoms. In **2**, one cyclopentadienyl ring [bound to Fe(2)] was found disordered over two positions and the site occupation factors were refined yielding the values 0.65 and 0.35, respectively. Some disorder was also detected in the CF$_3$SO$_3^-$ anion of *cis*-**8** for the fluorine and oxygen atoms which were refined over two sites yielding occupation factors of 0.70 and 0.50 for the main images of the O and F atoms, respectively. All hydrogen atoms, except the hydrogen bound to the C$_\beta$ carbon [C(4)] in complex **2** which was located in the Fourier map and refined isotropically, were added in calculated positions, included in the final stage of refinement with isotropic thermal parameters, $U(H) = 1.2U_{eq}(C)$ [$U(H) = 1.5U_{eq}(C–Me)$], and allowed to ride on their carrier carbons. Crystal data and details of the data collection for all structures are reported in Table 3. SCHAKAL97 has been used for the graphical representations [17].

5. Supplementary material

Crystallographic data for the structural analyses have been deposited with the Cambridge Crystallographic Data Centre, CCDC no. 216794 for **2**, no. 216795 for *trans*-**8** and 216796 for *cis*-**8**. Copies of this information can be obtained free of charge from the Director, CCDC, 12 Union Road, Cambridge CB2 1EZ, UK (fax: +44-1233-336033; deposit@ccdc.cam.ac.uk or www.ccdc.cam.ac.uk).

References

[1] V.G. Albano, L. Busetto, F. Marchetti, M. Monari, S. Zacchini, V. Zanotti, Organometallics 22 (2003) 1326.

[2] (a) Examples of vinyliminium complexes in different coordination modes include: D.J. Bernard, M.A. Esteruelas, A.M. Lopez, J. Modrego, M.C. Puerta, P. Valerga, Organometallics 18 (1999) 4995;
(b) N. Mantovani, L. Marvelli, R. Rossi, V. Bertolasi, C. Bianchini, I. de los Rios, M. Peruzzini, Organometallics 21 (2002) 2382;
(c) A.S. Gamble, P.S. White, J.L. Templeton, Organometallics 10 (1991) 693;
(d) C.J. Adams, K.M. Anderson, I.M. Bartlett, N.G. Connelly, A.G. Orpen, T.J. Paget, H. Phetmung, D.W. Smith, J. Chem. Soc., Dalton Trans. (2001) 1284;
(e) M.R. Churchill, C.H. Lake, R.A. Lashewycz-Rubycz, H. Yao, R.D. McCargar, J.B. Keister, J. Organomet. Chem. 452 (1993) 151;
(f) S. Aime, D. Osella, A.J. Deeming, A.J. Arce, J. Chem. Soc., Dalton Trans. (1986) 1459.

[3] (a) V.G. Albano, L. Busetto, C. Camiletti, C. Castellari, M. Monari, V. Zanotti, J. Chem. Soc., Dalton Trans. (1997) 4671;
(b) V.G. Albano, S. Bordoni, L. Busetto, C. Camiletti, M. Monari, A. Palazzi, F. Prestopino, V. Zanotti, J. Chem. Soc., Dalton Trans. (1997) 4665.

[4] (a) V.G. Albano, L. Busetto, F. Marchetti, M. Monari, V. Zanotti, J. Organomet Chem. 649 (2002) 64;
(b) V.G. Albano, L. Busetto, M. Monari, V. Zanotti, J. Organomet. Chem. 606 (2000) 163;
(c) V.G. Albano, S. Bordoni, L. Busetto, F. Marchetti, M. Monari, V. Zanotti, J. Organomet. Chem. 684 (2003) 37.

[5] (a) A.F. Dyke, S.A.R. Knox, P.J. Naish, G.E. Taylor, J. Chem. Soc., Chem.Commun. (1980) 409;
(b) D.L. Davies, A.F. Dyke, S.A.R. Knox, M.J. Morris, J. Organomet. Chem. 215 (1981) C30;
(c) A.F. Dyke, S.A.R. Knox, P.J. Naish, G.E. Taylor, J. Chem. Soc., Dalton Trans. (1982) 1297;
(d) B.P. Gracey, S.A.R. Knox, K.A. Macpherson, A.G. Orpen, S.R. Stobart, J. Chem. Soc., Dalton Trans. (1985) 1935.

[6] (a) V. Zanotti, S. Bordoni, L. Busetto, L. Carlucci, A. Palazzi, R. Serra, V.G. Albano, M. Monari, F. Prestopino, F. Laschi, P. Zanello, Organometallics 14 (1995) 5232;
(b) R.F. Bryan, P.T. Green, J. Chem. Soc. A (1970) 3064.

[7] (a) F.A. Cotton, G. Wilkinson, Advanced Inorganic Chemistry, fifth ed., Wiley, New York, 1988, pp. 1325–1327;
(b) R.D. Adams, F.A. Cotton, J. Am. Chem. Soc. 95 (1973) 6589.

[8] (a) C.P. Casey, K.P. Gable, D.M. Roddick, Organometallics 9 (1990) 221;
(b) N.C. Schroeder, R. Funchess, R.A. Jacobson, R.J. Angelici, Organometallics 8 (1989) 521;
(c) R.E. Colborn, D.L. Davies, A.F. Dyke, S.A.R. Knox, K.A. Mead, A.G. Orpen, J. Chem. Soc., Dalton Trans. (1989) 1799;
(d) R.E. Colborn, A.F. Dyke, S.A.R. Knox, K.A. Mead, P. Woodward, J. Chem. Soc., Dalton Trans. (1983) 2099.

[9] N.A. Guillevic, E.L. Hancox, B.E. Mann, J. Chem. Soc., Dalton Trans. (1992) 1729.

[10] A.F. Dyke, S.A.R. Knox, M. Morris, P.J. Naish, J. Chem. Soc., Dalton Trans. (1983) 1417.

[11] K. Stott, J. Stonehouse, J. Keeler, T.L. Hwang, A.J. Shaka, J. Am. Chem. Soc. 117 (1995) 4199.

[12] (a) G. Cox, C. Dowling, A.R. Manning, P. McArdle, D. Cunningham, J. Organomet. Chem. 438 (1992) 143;
(b) K. Boss, C. Dowling, A.R. Manning, J. Organomet. Chem. 509 (1996) 19.

[13] SMART & SAINT Software Reference Manuals, version 5.051 (Windows NT Version), Bruker Analytical X-ray Instruments Inc.: Madison, Wi, 1998.

[14] G.M. Sheldrick, SADABS, program for empirical absorption correction, University of Göttingen, Germany, 1996.

[15] A. Altomare, G. Cascarano, C. Giacovazzo, A. Guagliardi, A.G.G. Moliterni, M.C. Burla, G. Polidori, M. Camalli, D. Siliqi, Acta Crystallogr., Sect. A 52 (1996) C79.

[16] G.M. Sheldrick, SHELXTLplus (Windows NT Version) Structure Determination Package Version 5.1, Bruker Analytical X-ray Instruments, Madison, WI, USA, 1998.

[17] E. Keller, SCHAKAL97, Graphical Representation of Molecular Models, University of Freiburg, Germany, 1997.